Hindawi Publishing Corporation
EURASIP Journal on Wireless Communications and Networking
Volume 2009, Article ID 957159, 11 pages
doi:10.1155/2009/957159

Research Article

On the Information Rate of Single-Carrier FDMA Using Linear Frequency Domain Equalization and Its Application for 3GPP-LTE Uplink

Hanguang Wu,[1] Thomas Haustein (EURASIP Member),[2] and Peter Adam Hoeher[3]

[1] *COO RTP PT Radio System Technology, Nokia Siemens Networks, St. Martin Street 76, 81617 Munich, Germany*
[2] *Fraunhofer Institute for Telecommunications, Heinrich Hertz Institute, Einsteinufer 37, 10587 Berlin, Germany*
[3] *Faculty of Engineering, University of Kiel, Kaiserstraße 2, 24143 Kiel, Germany*

Correspondence should be addressed to Hanguang Wu, wuhanguang@gmail.com

Received 31 January 2009; Revised 25 May 2009; Accepted 19 July 2009

Recommended by Bruno Clerckx

This paper compares the information rate achieved by SC-FDMA (single-carrier frequency-division multiple access) and OFDMA (orthogonal frequency-division multiple access), where a linear frequency-domain equalizer is assumed to combat frequency selective channels in both systems. Both the single user case and the multiple user case are considered. We prove analytically that there exists a rate loss in SC-FDMA compared to OFDMA if decoding is performed independently among the received data blocks for frequency selective channels. We also provide a geometrical interpretation of the achievable information rate in SC-FDMA systems and point out explicitly the relation to the well-known waterfilling procedure in OFDMA systems. The geometrical interpretation gives an insight into the cause of the rate loss and its impact on the achievable rate performance. Furthermore, motivated by this interpretation we point out and show that such a loss can be mitigated by exploiting multiuser diversity and spatial diversity in multi-user systems with multiple receive antennas. In particular, the performance is evaluated in 3GPP-LTE uplink scenarios.

1. Introduction

In high data rate wideband wireless communication systems, OFDM (orthogonal frequency-division multiplexing) and SC-FDE (single-carrier system with frequency domain equalization), are recognized as two popular techniques to combat the frequency selectivity of the channel. Both techniques use block transmission and employ a cyclic prefix at the transmitter which ensures orthogonality and enables efficient implementation of the system using the fast Fourier transform (FFT) and one tap scalar equalization per subcarrier at the receiver. There has been a long discussion on a comparison between OFDM and SC-FDE concerning different aspects [1–3]. In order to accommodate multiple users in the system, OFDM can be straightforward extended to a multiaccess scheme called OFDMA, where each user is assigned a different set of subcarriers. However, an extension to an SC-FDE based multiaccess scheme is not obvious and it has been developed only recently, called single-carrier FDMA (SC-FDMA) [4]. (A single-carrier waveform can only be obtained for some specific sub-carrier mapping constraints. In this paper we do not restrict ourself to these constraints but refer SC-FDMA to as DFT-precoded OFDMA with arbitrary sub-carrier mapping.) SC-FDMA can be viewed as a special OFDMA system with the user's signal pre-encoded by discrete Fourier transform (DFT), hence also known as DFT-precoded OFDMA or DFT-spread OFDMA. One prominent advantage of SC-FDMA over OFDMA is the lower PAPR (peak-to-average power ratio) of the transmit waveform for low-order modulations like QPSK and BPSK, which benefits the mobile users in terms of power efficiency [5]. Due to this advantage, recently SC-FDMA has been agreed on to be used for 3GPP LTE uplink transmission [6]. (LTE (Long Term Evolution) is the evolution of the 3G mobile network standard UMTS (Universal Mobile Telecommunications System) defined by the 3rd Generation

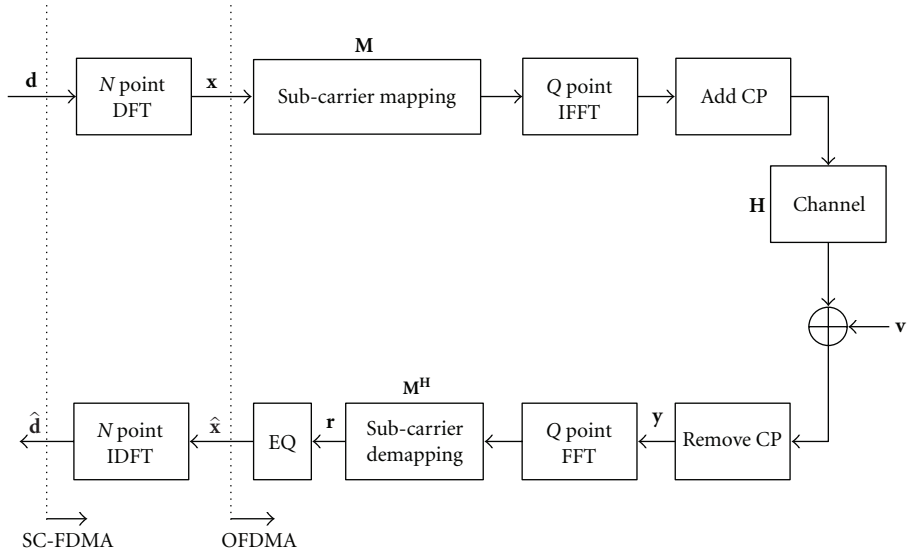

Figure 1: Block diagram of SC-FDMA systems and its relation to OFDMA systems.

Partnership Project (3GPP).) In order to obtain a PAPR comparable to the conventional single carrier waveform in the SC-FDMA transmitter, sub-carriers assigned to a specific user should be adjacent to each other [7] or equidistantly distributed over the entire bandwidth [8], where the former is usually referred to as localized mapping and the latter distributed mapping.

This paper investigates the achievable information rate using SC-FDMA in the uplink. We present a framework for analytical comparison between the achievable rate in SC-FDMA and that in OFDMA. In particular, we compare the rate based on a widely used transmission structure in both systems, where equal power allocation (meaning a flat power spectral density mask) is used for the transmitted signal of each user, and linear frequency domain equalization is employed at the receiver.

The fact that OFDMA decomposes the frequency-selective channel into parallel AWGN sub-channels suggests a separate coding for each sub-channel without losing channel capacity, where independent near-capacity-achieving AWGN codes can be used for each sub-channel and accordingly the received signal is decoded independently among the sub-channels. This communication structure is of high interest both in communication theory and in practice, since near-capacity-achieving codes (e.g., LDPC and Turbo codes) have been well studied for the AWGN channel. We show that although SC-FDMA can be viewed as a collection of virtual Gaussian sub-channels, these sub-channels are correlated; hence separate coding and decoding for each of them is not sufficient to achieve channel capacity. We further investigate the achievable rate in SC-FDMA if a separate capacity-achieving AWGN code for each sub-channel is used subject to equal power allocation of the transmitted signal. The special case that all the sub-carriers are exclusively utilized by a single user, that is, SC-FDE, is investigated in [3], and it is shown that the SC-FDE rate is always lower than the OFDM rate in frequency selective channels. However, an insight into the cause of the rate loss and its impact on the performance was not given. Such an insight is of interest and importance to design appropriate transmission strategies in SC-FDMA systems, where a number of sub-carriers and multi-users or possibly multiple antennas are involved. In this paper, based on the property of the circular matrix we derive a framework of rate analysis for SC-FDMA and OFDMA, which is a generalization of the result in [3], and it allows for the calculation of the achievable rate using arbitrary sub-carrier assignment methods in both the single user system and the multi-user system subject to individual power constraints of the users. We analyze the cause of the rate loss and its impact on the achievable rate as well as provide the geometrical interpretation of the achievable rate in SC-FDMA. Moreover, we reveal an interesting relation between the geometrical interpretation and the well-known waterfilling procedure in OFDMA systems. More importantly, motivated by this geometrical interpretation we show that such a loss can be mitigated by exploiting multi-user diversity and spatial diversity in the multi-user system with multiple receive antennas, which is usually available in mobile systems nowadays.

The paper is organized as follows. In Section 2 we introduce the system model and the information rate for OFDMA and SC-FDMA. In Section 3 we derive the SC-FDMA rate result and provide its geometrical interpretation assuming equal power allocation without joint decoding. Then we extend and discuss the SC-FDMA rate result for the multi-user case and for multi-antenna systems in Section 4. Simulation results are given in Section 5, and conclusions are drawn in Section 6.

2. System Model and Information Rate

Consider the SC-FDMA uplink transmission scheme depicted in Figure 1. The only difference from OFDMA is

the addition of the N point DFT at the transmitter and the N point IDFT at the receiver. The transmitted signal block $\mathbf{d} = [d_0, \ldots, d_{N-1}]^T$ of size N spreads onto the N sub-carriers selected by the sub-carrier mapping method. In other words, the transmitted signal vector is pre-encoded by DFT before going to the OFDMA modulator. For OFDMA transmission, a specific set of sub-carriers is assigned to the user through the sub-carrier mapping stage. Then multi-carrier modulation is performed via a Q point IFFT ($Q > N$), and a cyclic prefix (CP) longer than the maximum channel delay is inserted to avoid interblock interference. The frequency selective channel can be represented by a tap delay line model with the tap vector $\mathbf{h} = [h_0, h_1, \ldots, h_L]^T$ and the additive white Gaussian noise (AWGN) $\mathbf{v} \sim \mathcal{N}(0, N_0)$. At the receiver, the CP is removed and a Q point FFT is performed. A demapping procedure consisting of the spectral mask of the desired user is then applied, followed by zero forcing equalization which involves a scalar channel inversion per sub-carrier. For SC-FDMA, the equalized signal is further transformed to the time domain using an N point IDFT where decoding and detection take place.

In the following, we first briefly review the achievable sum rate in the OFDMA system and then show the sum rate relationship between OFDMA and SC-FDMA. We assume in the uplink that the users' channels are perfectly measured by the base station (BS), where the resource allocation algorithm takes place and its decision is then sent to the users via a signalling channel in the downlink. For simplicity, we start with the single-user single-input single-output system and then extend it to the multi-user case with multiple antennas at the BS. For convenience, the following notations are employed throughout the paper. $\mathbf{F_N}$ is the $N \times N$ Fourier matrix with the (n,k)th entry $[\mathbf{F_N}]_{n,k} = (1/\sqrt{N})e^{-j2\pi nk/N}$, and $\mathbf{F_N^H}$ denotes the inverse Fourier matrix. Further on, the assignment of data symbols x_n to specific sub-carriers is described by the $Q \times N$ sub-carrier mapping matrix $\mathbf{M}$ with the entry

$$m_{q,n} = \begin{cases} 1, & \text{if the } n\text{th data is assigned to the } q\text{th sub-carrier} \\ 0, & \text{otherwise,} \end{cases} \tag{1}$$

$0 \le q \le Q-1,\ 0 \le n \le N-1.$

2.1. OFDMA Rate. After CP removal at the receiver, the received block can be written as

$$\mathbf{y} = \mathbf{H}\mathbf{F_Q^H}\mathbf{M}\mathbf{x} + \mathbf{v}, \tag{2}$$

where $\mathbf{x} = [x_0, \ldots, x_{N-1}]$ is the transmitted block of the OFDMA system, and $\mathbf{H}$ is a $Q \times Q$ circulant matrix with the first column $\mathbf{h} = [h_0, \ldots, h_{L-1}, 0, \ldots, 0]^T$. The following discussion makes use of the important properties of circulant matrices given in the appendices (Facts 1 and 2). Performing multi-carrier demodulation using FFT and sub-carrier demapping using $\mathbf{M^H}$, we obtain the received block

$$\mathbf{r} = \mathbf{M^H}\mathbf{F_Q}\mathbf{y} = \mathbf{M^H}\mathbf{F_Q}\mathbf{H}\mathbf{F_Q^H}\mathbf{M}\mathbf{x} + \mathbf{M^H}\mathbf{F_Q}\mathbf{v} \tag{3}$$

$$= \mathbf{M^H}\mathbf{D}\mathbf{M}\mathbf{x} + \mathbf{M^H}\mathbf{F_Q}\mathbf{v} \tag{4}$$

$$= \mathbf{M^H}\mathbf{M}\boldsymbol{\Lambda}\mathbf{x} + \mathbf{M^H}\mathbf{F_Q}\mathbf{v} \tag{5}$$

$$= \boldsymbol{\Lambda}\mathbf{x} + \boldsymbol{\eta}, \tag{6}$$

where Fact 1 (see Appendix A) is used from step (3) to (4) and $\mathbf{D} = \mathbf{F_Q}\mathbf{H}\mathbf{F_Q^H} = \mathrm{diag}\{\widetilde{\mathbf{h}}\}$ with the diagonal entries being the frequency response of the channel. The step (4) to (5) follows from the equality

$$\mathbf{D}\mathbf{M} = \mathbf{M}\boldsymbol{\Lambda}, \tag{7}$$

where $\boldsymbol{\Lambda} = \mathrm{diag}\{\hat{h}_0, \hat{h}_1, \ldots, \hat{h}_{N-1}\}$ is an $N \times N$ diagonal matrix with its diagonal entries being the channel frequency response at the selected sub-carriers of the user. This relationship can be readily verified since $\mathbf{M}$ has only a single nonzero unity entry per column, and this structure of $\mathbf{M}$ also leads to

$$\mathbf{M^H}\mathbf{M} = \mathbf{I_N}, \tag{8}$$

with which we arrive at step (6). The $N \times 1$ vector $\boldsymbol{\eta} = \mathbf{M^H}\mathbf{F_Q}\mathbf{v}$ is a linear transformation of $\mathbf{v}$, and hence it remains Gaussian whose covariance matrix is given by

$$E\{\boldsymbol{\eta}\boldsymbol{\eta}^{\mathbf{H}}\} = E\left\{\mathbf{M^H}\mathbf{F_Q}\mathbf{v}\mathbf{v}^{\mathbf{H}}\mathbf{F_Q^H}\mathbf{M}\right\}$$

$$= \mathbf{M^H}\underbrace{\mathbf{F_Q}E\{\mathbf{v}\mathbf{v}^{\mathbf{H}}\}\mathbf{F_Q^H}}_{\mathrm{N_0I_Q}}\mathbf{M} \tag{9}$$

$$= N_0\mathbf{M^H}\mathbf{I_Q}\mathbf{M} \tag{10}$$

$$= N_0\mathbf{M^H}\mathbf{M}\mathbf{I_N} \tag{11}$$

$$= N_0\mathbf{I_N}, \tag{12}$$

where the step (9) to (10) follows from Fact 2 (see Appendix A), (10) to (11) follows from (7) since $\mathbf{I_Q}$ is also a diagonal matrix, and the step (11) to (12) results from (8). Therefore, $\boldsymbol{\eta}$ is a vector consisting of uncorrelated Gaussian noise samples. The frequency domain ZF equalizer is given by the inverse of the diagonal matrix $\boldsymbol{\Lambda}^{-1}$ which essentially preserves the mutual information provided that $\boldsymbol{\Lambda}$ is invertible. Here we assume that $\boldsymbol{\Lambda}$ is always invertible since the BS can avoid assigning sub-carriers with zero channel frequency response to the user. Due to the diagonal structure of $\boldsymbol{\Lambda}$ and independent noise samples of $\boldsymbol{\eta}$ (uncorrelated Gaussian samples are also independent), (6) can be viewed as the transmit signal components or the data symbols on the assigned sub-carriers propagating through independent Gaussian sub-channels with different gains. This structure suggests that coding can be done independently for each sub-channel to asymptotically achieve the channel capacity. The only loss is due to the cyclic prefix overhead relative to the transmit signal block length. The achievable sum rate of an

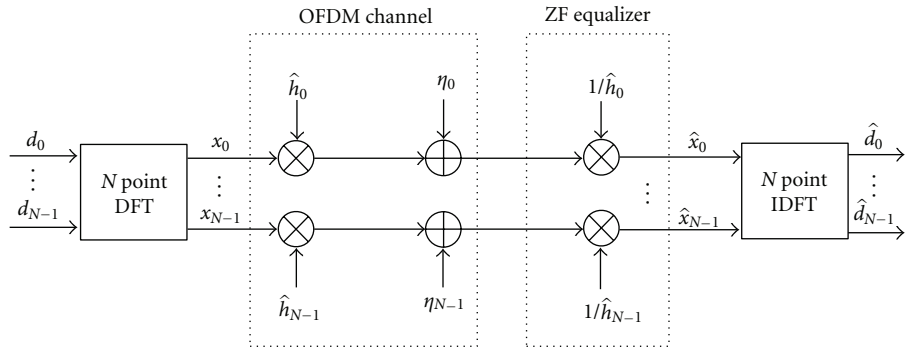

Figure 2: Equivalent block diagram of SC-FDMA systems.

OFDMA system can be calculated as the sum of the rates of the assigned sub-carriers, which is given by

$$C_{\text{OFDMA}} = \sum_{n=0}^{N-1} \log_2\left(1 + \frac{P_n \left|\hat{h}_n\right|^2}{N_0}\right), \tag{13}$$

where P_n is the power allocated to the nth sub-carrier. Note that the employment of a zero forcing (ZF) equalizer performing channel inversion for each sub-carrier preserves the capacity since the resulting signal-to-noise ratio (SNR) for each sub-carrier remains unchanged. To maximize the OFDMA rate subject to the total transmit power constraint P_{total}, the assignment of the transmit power to the n independent Gaussian sub-channels should follow the waterfilling principle, and so the optimal power P_n of the nth sub-carrier is given by

$$P_n = \max\left(0, \lambda - \frac{N_0}{\left|\hat{h}_n\right|^2}\right), \tag{14}$$

where the positive constant λ must be chosen in order to fulfill the total transmit power constraint

$$P_{\text{total}} = \text{tr}\{\mathbf{x}\mathbf{x}^{\mathbf{H}}\} = \sum_{n=0}^{N-1} \max\left(0, \lambda - \frac{N_0}{\left|\hat{h}_n\right|^2}\right), \tag{15}$$

where $\text{tr}\{\cdot\}$ stands for the trace of the argument. It should be noted that the waterfilling procedure implicitly selects the optimal sub-carriers out of the available sub-carriers in the system and assigns optimal transmit power to each of them. Therefore, it is possible that some sub-carriers are not used. In our model, the waterfilling procedure amounts to mapping $\mathbf{x}$ to the desired sub-carriers and at the same time constructing $\mathbf{x}$ having diagonal covariance matrix $\mathbf{R}_{\mathbf{x}} = \text{diag}\{P_0, P_1, \ldots, P_{N-1}\}$ with entries equal to the optimal power allocated to the desired sub-carriers.

2.2. SC-FDMA Rate. OFDMA converts the frequency selective channels into independent AWGN channels with different gains. Therefore, a block diagram of SC-FDMA can be equivalently regarded as applying DFT precoding for parallel AWGN channels and performing IDFT decoding after equalization as illustrated in Figure 2. The output of the IDFT can be derived as

$$\begin{aligned}\hat{\mathbf{d}} &= \mathbf{F}_{\mathbf{N}}^{\mathbf{H}}\boldsymbol{\Lambda}^{-1}\mathbf{r} = \mathbf{F}_{\mathbf{N}}^{\mathbf{H}}\boldsymbol{\Lambda}^{-1}\boldsymbol{\Lambda}\mathbf{x} + \mathbf{F}_{\mathbf{N}}^{\mathbf{H}}\boldsymbol{\Lambda}^{-1}\boldsymbol{\eta} \\ &= \mathbf{F}_{\mathbf{N}}^{\mathbf{H}}\boldsymbol{\Lambda}^{-1}\boldsymbol{\Lambda}\mathbf{F}_{\mathbf{N}}\mathbf{d} + \mathbf{F}_{\mathbf{N}}^{\mathbf{H}}\boldsymbol{\Lambda}^{-1}\boldsymbol{\eta} \\ &= \mathbf{d} + \mathbf{F}_{\mathbf{N}}^{\mathbf{H}}\boldsymbol{\Lambda}^{-1}\boldsymbol{\eta} \\ &= \mathbf{d} + \hat{\boldsymbol{\eta}},\end{aligned} \tag{16}$$

where we denote $\hat{\boldsymbol{\eta}} = \mathbf{F}_{\mathbf{N}}^{\mathbf{H}}\boldsymbol{\Lambda}^{-1}\boldsymbol{\eta}$ by the residual noise vector after ZF equalizer and IDFT. With (16) the transmit data components in SC-FDMA system can be viewed as propagating through virtual sub-channels distorted by the amount of noise given by $\hat{\boldsymbol{\eta}}$. Note that $\hat{\boldsymbol{\eta}}$ is a Gaussian vector due to the linear transformation but it is entries are generally correlated which we show in the following:

$$\begin{aligned}\mathbf{R}_{\hat{\eta}} &= E\left\{\hat{\boldsymbol{\eta}}\hat{\boldsymbol{\eta}}^{\mathbf{H}}\right\} \\ &= E\left\{\mathbf{F}_{\mathbf{N}}^{\mathbf{H}}\boldsymbol{\Lambda}^{-1}\boldsymbol{\eta}\boldsymbol{\eta}^{\mathbf{H}}\boldsymbol{\Lambda}^{-\mathbf{H}}\mathbf{F}_{\mathbf{N}}\right\} \\ &= \mathbf{F}_{\mathbf{N}}^{\mathbf{H}}\boldsymbol{\Lambda}^{-1}E\{\boldsymbol{\eta}\boldsymbol{\eta}^{\mathbf{H}}\}\boldsymbol{\Lambda}^{-\mathbf{H}}\mathbf{F}_{\mathbf{N}} \\ &= N_0\mathbf{F}_{\mathbf{N}}^{\mathbf{H}}\boldsymbol{\Lambda}^{-1}\boldsymbol{\Lambda}^{-\mathbf{H}}\mathbf{F}_{\mathbf{N}} \qquad (17) \\ &= N_0\underbrace{\mathbf{F}_{\mathbf{N}}^{\mathbf{H}}\underbrace{|\boldsymbol{\Lambda}|^{-2}}_{\text{diagonal}}\mathbf{F}_{\mathbf{N}}}_{\text{circulant}}, \qquad (18)\end{aligned}$$

where $|\cdot|$ is applied to $\boldsymbol{\Lambda}$ elementwise, and the step from (17) to (18) follows from the fact that $\boldsymbol{\Lambda}$ is a diagonal matrix. The matrix $|\boldsymbol{\Lambda}|^{-2}$ is hence also diagonal with the diagonal entries being the reciprocal of channel power gains of the assigned sub-carriers of the user, which are usually not equal in frequency selective channels. Hence $\mathbf{R}_{\hat{\eta}}$ is a circulant matrix according to Fact 2 (see Appendix A) with nonzero values on the off diagonal entries. Therefore, the residual noise on the virtual sub-channels is correlated and hence SC-FDMA does not have the same parallel AWGN sub-channel representation as OFDMA. However, note that the DFT at the SC-FDMA transmitter does not change the total transmit

power due to the property of the Fourier matrix $\mathbf{F^H F} = \mathbf{I}$, that is,

$$P_{\mathbf{x}} = \mathbf{x^H x} = \mathbf{d^H F^H F d} = \mathbf{d^H d} = P_{\mathbf{d}}. \tag{19}$$

The property of power conservation of the DFT precoder at the transmitter and invertibility of IDFT at the receiver leads to the conclusion that the mutual information is preserved. Hence, the mutual information between the transmit vector and post-detection vector $I(\mathbf{d}, \hat{\mathbf{d}})$ is equal to that of OFDMA $I(\mathbf{x}, \hat{\mathbf{x}})$. In other words, for any sub-carrier mapping and power allocation methods in OFDMA system, there exists a corresponding configuration in SC-FDMA which achieves the same rate as OFDMA. For example, suppose, for a given time invariant frequency selective channel, that $\mathbf{R_x}$ is the optimal covariance matrix given by the waterfilling solution in an OFDMA system. To obtain the same rate in an SC-FDMA system, the covariance matrix of the transmitted signal $\mathbf{R_d}$ can be designed as

$$\mathbf{R_d} = E\{\mathbf{dd^H}\} = E\{\mathbf{F^H x x^H F}\} = \underbrace{\mathbf{F^H} \underbrace{E\{\mathbf{xx^H}\}}_{\text{diag}\{\mathbf{p}\}} \mathbf{F}}_{\text{circulant}\{\hat{\mathbf{p}}\}}, \tag{20}$$

where in the last step we use Fact 2 (see Appendix A). Hence, $\mathbf{R_d}$ is a circulant matrix with the first column $\hat{\mathbf{p}} = (1/\sqrt{N})\mathbf{F^H p}$. Since both the covariance matrix of the transmitted signal and residual noise exhibit a circulant structure in an SC-FDMA system, correlation exists in both the transmitted symbols before DFT and the received symbols after IDFT. Such correlation complicates the code design problem in order to achieve the same rate as in OFDMA. This paper makes no attempt to design a proper coding scheme for SC-FDMA but we mention that SC-FDMA is not inferior to OFDMA regarding the achievable information rate from an information theoretical point of view. Instead, it can achieve the same rate as OFDMA if proper coding is employed. Note that the above statement implies using the same sub-carriers to convey information in both systems. Therefore, SC-FDMA and OFDMA are the same regarding the rate if they both use the same sub-carrier and the same corresponding power for each sub-carrier to convey information. However, in SC-FDMA coding and decoding should be applied across the transmitted and received signal components, respectively.

3. SC-FDMA Rate Using Equal Power Allocation without Joint Decoding

The waterfilling procedure discussed above is computationally complex which requires iterative sub-carrier and power allocation in the system. An efficient sub-optimal approach with reduced complexity is to use equal power allocation across a properly chosen subset of sub-carriers [9], which is shown to have very close performance to the waterfilling solution. In other words, this approach assumes $E\{\mathbf{xx^H}\} = (P_{\text{total}}/N)\mathbf{I} \triangleq P_e\mathbf{I}$ and designs a proper sub-carrier mapping matrix to approximate the waterfilling solution, where the number of used sub-channels N is also a design parameter. This approach can also be applied to an SC-FDMA system to approximate the waterfilling solution since DFT precoding and decoding are information lossless according to our discussion in Section 2. Note that DFT precoding does not change the equal power allocation property of the transmitted signal according to Fact 2 (see Appendix A), that is, $E\{\mathbf{dd^H}\} = E\{\mathbf{xx^H}\} = P_e\mathbf{I}$ ($P_{\mathbf{x}} = P_{\mathbf{d}} = P_{\text{total}}$). Therefore, to obtain the same rate as in OFDMA, coding does not need to be applied across transmitted signal components, and only correlation among the received signal components needs to be taken into account for decoding.

3.1. SC-FDMA Rate without Joint Decoding. We are interested to see what the achievable rate in SC-FDMA is if a capacity-achieving AWGN code is used for each transmitted component, which is decoded independently at the receiver. Under the above given condition, the achievable rate in SC-FDMA is the sum of the rate of each virtual subchannel for which we need to calculate the post-detection SNR, that is, the post-detection SNR of the nth virtual subchannel can be expressed as

$$\begin{aligned}
\gamma_{\text{SC-FDMA},n} &= \frac{P_e}{E\left\{\hat{\boldsymbol{\eta}}\hat{\boldsymbol{\eta}}^{\mathbf{H}}\right\}_{n,n}} = \frac{P_e}{N_0\left(\sum_{n=0}^{N-1}\left(1/\left|\hat{h}_n\right|^2\right)\right)/N} \\
&= \frac{NP_e}{N_0\left(\sum_{n=0}^{N-1}\left(1/\left|\hat{h}_n\right|^2\right)\right)} \\
&= \frac{HM\left(\hat{h}_n\right)\cdot P_e}{N_0} \qquad (21) \\
&= \gamma. \qquad (22)
\end{aligned}$$

In step (21) we denote $HM(|\hat{h}_n|^2) = N/\sum_{n=0}^{N-1}(1/|\hat{h}_n|^2)$ which is the harmonic mean of $|\hat{h}_n|^2, (n = 0, \ldots, N-1)$ by definition. In the last step we let $\gamma = (HM(|\hat{h}_n|^2)\cdot P_e)/N_0$ since the post-detection SNR is equal for all the virtual subchannels. Using Shannon's formula the achievable rate in SC-FDMA can be obtained as

$$\begin{aligned}
C_{\text{SC-FDMA}}^{\text{EP, Independent}} &= N\log_2(1+\gamma) \\
&= N\log_2\left(1 + \frac{HM\left(\left|\hat{h}_n\right|^2\right)\cdot P_e}{N_0}\right),
\end{aligned} \tag{23}$$

which is a function of the harmonic mean of the power gains at the assigned sub-carriers. Note that the result in [3] is a special case of (23) where all the available sub-carriers in the system are used by the user. It is perceivable that $C_{\text{SC-FDMA}}^{\text{EP,Independent}} \leq C_{\text{OFDM}}^{\text{EP}}$ because noise correlation between the received components is not exploited to recover

the signal. In the following, we will prove this inequality analytically. In order to prove

$$N\log_2\left(1+\frac{HM\left(\left|\hat{h}_n\right|^2\right)\cdot P_e}{N_0}\right)\le\sum_{n=0}^{N-1}\log_2\left(1+\frac{\left|\hat{h}_n\right|^2P_e}{N_0}\right), \tag{24}$$

it is equivalent to prove

$$\left(1+\frac{HM\left(\left|\hat{h}_n\right|^2\right)\cdot P_e}{N_0}\right)^N\le\prod_{n=0}^{N-1}\left(1+\frac{\left|\hat{h}_n\right|^2P_e}{N_0}\right), \tag{25}$$

since $\log_2(\cdot)$ is a monotonically increasing function. Because the term $(1+(|\hat{h}_n|^2P_e)/N_0)$ is positive and the geometric mean of positive values is not less than the harmonic mean, we have

$$\left(\prod_{n=0}^{N-1}\left(1+\frac{\left|\hat{h}_n\right|^2P_e}{N_0}\right)\right)^{1/N}\ge\frac{N}{\sum_{n=0}^{N-1}\left(1/\left(1+\left(\left|\hat{h}_n\right|^2P_e\right)/N_0\right)\right)}. \tag{26}$$

The Hoehn-Niven theorem [10] states the following: Let $HM(\cdot)$ be the harmonic mean and let $a_1,a_2,\ldots,a_m,x$ be the positive numbers, where the a_i's are not all equal, then

$$HM(x+a_1,x+a_2,\ldots,x+a_m)>x+HM(a_1,a_2,\ldots,a_m) \tag{27}$$

holds. If we let $a_n=(|\hat{h}_n|^2P_e)/N_0$, for all n and $x=1$, by applying (27) we have

$$\frac{N}{\sum_{n=0}^{N-1}\left(1/\left(1+\left(\left|\hat{h}_n\right|^2P_e\right)/N_0\right)\right)}>1+HM\left(\frac{\left|\hat{h}_n\right|^2P_e}{N_0}\right)=1+HM\left(\left|\hat{h}_n\right|^2\right)\frac{P_e}{N_0}, \tag{28}$$

where the last step follows from the fact that P_e/N_0 is a constant value so that it can be factored out of the $HM(\cdot)$ operation. Therefore, by applying the transitive property of inequality to (26) and (28) it follows that

$$\left(\prod_{n=0}^{N-1}\left(1+\frac{\left|\hat{h}_n\right|^2P_e}{N_0}\right)\right)^{1/N}>1+HM\left(\left|\hat{h}_n\right|^2\right)\frac{P_e}{N_0}, \tag{29}$$

and taking the Nth power on both sides of (29), we have

$$\left(1+\frac{HM\left(\left|\hat{h}_n\right|^2\right)\cdot P_e}{N_0}\right)^N<\prod_{n=0}^{N-1}\left(1+\frac{\left|\hat{h}_n\right|^2P_e}{N_0}\right). \tag{30}$$

By definition, it is easy to prove that if all the $|\hat{h}_n|^2, n=0,\ldots,N-1$ are equal, $HM(|\hat{h}_n|^2)=|\hat{h}_n|^2$ holds and thus

$$\left(1+\frac{HM\left(\left|\hat{h}_n\right|^2\right)\cdot P_e}{N_0}\right)^N=\prod_{n=0}^{N-1}\left(1+\frac{\left|\hat{h}_n\right|^2P_e}{N_0}\right) \tag{31}$$

holds, which corresponds to the case of frequency flat fading. Therefore, (24) holds in general.

The harmonic mean is sensitive to a single small value. $HM(|\hat{h}_n|^2)$ tends to be small if one of the values $|\hat{h}_n|^2$ is small. Therefore, the achievable sum rate in SC-FDMA depending on the harmonic mean of the power gain of the assigned sub-carriers would be sensitive to one single deep fade whose sub-carrier power gain is small. To give an intuitive impression how sensitive it is, we make use of the geometrical interpretation of the harmonic mean by Pappus of Alexandria [11] which is provided in Appendix B.

3.2. Relation to OFDMA. In the following, we will show that the achievable sum rate of SC-FDMA using equal power allocation without joint decoding is equivalent to that achieved by nonprecoded OFDMA system with equal gain power (EGP) allocation among the assigned sub-carriers. This conclusion will lead to our geometrical interpretation of the SC-FDMA system.

In an OFDMA system, the EGP allocation strategy pre-equalizes the transmitted signal so that all gains of the assigned sub-carriers are equal, that is,

$$P_n\frac{\left|\hat{h}_n\right|^2}{N_0}=\text{constant},\quad\forall n,\qquad\text{subject to }\sum_n P_n=P_{\text{total}}, \tag{32}$$

which requires the power allocated to the nth assigned sub-carrier $P_{eg,n}$ to be

$$P_{eg,n}=\frac{P_{\text{total}}}{\left|\hat{h}_n\right|^2\sum_{n=0}^{N-1}\left(1/\left|\hat{h}_n\right|^2\right)}. \tag{33}$$

Upon insertion of (33) into (13), the achievable sum rate using EGP can be calculated as

$$C_{\text{OFDMA}}^{\text{EGP}}=N\log_2\left(1+\frac{P_{\text{total}}}{\sum_{n=0}^{N-1}\left(1/\left|\hat{h}_n\right|^2\right)}\right)=N\log_2\left(1+\frac{HM\left(\left|\hat{h}_n\right|^2\right)\cdot P_e}{N_0}\right), \tag{34}$$

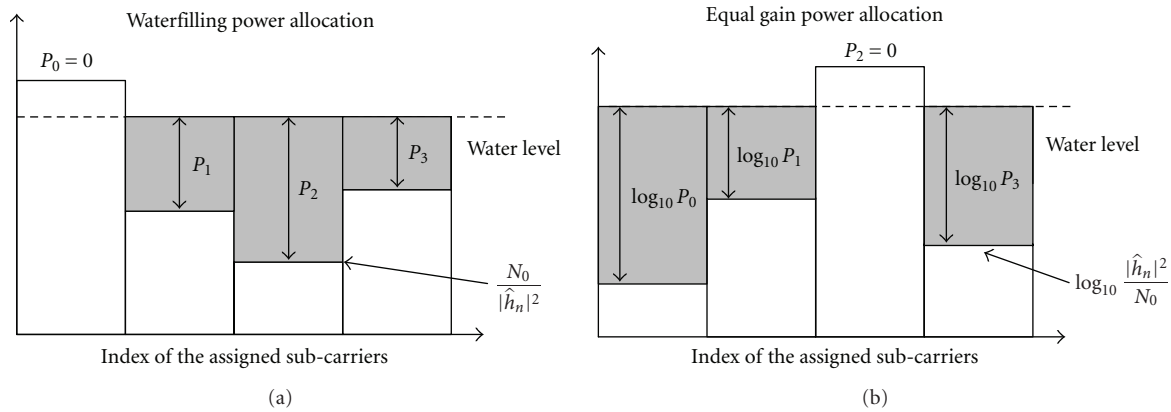

Figure 3: Comparison of geometrical interpretation between the waterfilling power allocation (a) and equal gain power allocation (b).

which is equal to $C_{\text{SC-FDMA}}^{\text{EP, Independent}}$ in (23), provided that both the SC-FDMA and OFDMA systems use the same assigned sub-carriers. This result leads to the conclusion that ZF equalized SC-FDMA with equal power allocation can be viewed as a nonprecoded OFDMA system performing EGP allocation among the assigned sub-carriers. It is worthy to point out that we find that EGP allocation shares a similar geometrical interpretation with waterfilling. This statement can be proven by applying logarithmic operation at both sides of the objective function of (32), which becomes

$$\begin{aligned} \log_{10} P_n + \log_{10}\left(\frac{\left|\hat{h}_n\right|^2}{N_0}\right) &= \log_{10}(\text{constant}) \\ &= \text{constant}, \quad \forall n \\ \text{subject to } \sum_n P_n &= P_{\text{total}}, \end{aligned} \tag{35}$$

where the objective function can be interpreted as shown in Figure 3(b): we can imagine that the quantity $\log_{10}(|\hat{h}_n|^2/N_0)$ is the bottom of a container and a fixed amount of water (power), P_{total}, is poured into the container. The water will then distribute inside the container to maintain a water level, denoted as constant in (35). Then the distance between the container bottom and the water level, that is, $\log_{10} P_n$, represents the power allocated to the nth assigned sub-carrier. Note that the waterfilling interpretation of EGP differs from the conventional waterfilling procedure of (14) in that firstly the container bottom is the inverse of that of the conventional waterfilling, and secondly the container bottom and the resulting power allocated to the individual sub-carrier should be measured in decibel. With the waterfilling interpretation of EGP it is possible to visualize how power is distributed among selected sub-carriers for ZF equalized SC-FDMA and also explain why putting power into weak sub-channels wastes so much capacity. Due to the inverse property of the container bottom, EGP allocates a larger portion of power to weaker sub-carriers and a smaller portion of power to stronger sub-carriers, which is opposite to the conventional waterfilling solution. Therefore, in order to achieve a higher data rate in SC-FDMA, it is important not to include weaker sub-carriers for communication because larger amount of power would be "wasted" in those sub-carriers. This observation suggests using strong sub-carriers for communication where an optimal sub-carrier allocation method, that is, optimal EGP allocation, is proposed in [12]. In frequency selective channels, such strong sub-carriers are usually not to be found adjacent to each other or equidistantly distributed over the entire bandwidth. Therefore, the sub-carrier mapping constraints to maintain the nice low PAPR for SC-FDMA has to be compromised if the optimal EGP allocation is applied. Within the scope of the work, we do not investigate such trade-off between the PAPR reduction and rate maximization. Instead, we will discuss in the following section that it is possible to obtain comparable rate performance as OFDMA and low PAPR as the single carrier waveform at the same time if multiple antennas are available at the BS.

4. Extension to Multiuser Case and Multiantenna Systems

The information rate analysis in Sections 2 and 3 assumes only one user in the system. However, the principle also holds for the multi-user case where each user's signal will be first individually precoded by DFT and then mapped to a different set of sub-carriers. It is known that in the multi-user OFDMA system, the maximum sum rate of all the users can be obtained by the multi-user waterfilling solution [13] where each user subject to an individual power constraint is assigned a different set of sub-carriers associated with a given power. Therefore, the information rate achieved in the system can be calculated as a sum of rate of each user, which can again be calculated similarly as in the single-user system. As a result, a multi-user SC-FDMA system can achieve the same rate as a multi-user OFDMA system since DFT and IDFT essentially preserve the mutual information of each user if the same resource allocation is assumed. If equal power allocation of the transmitted signal without joint decoding is assumed for each user, the system sum

rate $C_{\text{SC-FDMA,MU}}^{\text{EP,Independent}}$ of U users can be straightforward extended from (23), that is,

$$C_{\text{SC-FDMA,MU}}^{\text{EP, Independent}} = \sum_{u=1}^{U} N_u \log_2(1+\gamma_u) = \sum_{u=1}^{U} N_u \log_2\left(1+\frac{HM\left(\left|\hat{h}_{n,u}\right|^2\right)\cdot P_{n,u}}{N_0}\right), \tag{36}$$

where N_u is the length of the transmitted signal block of the uth user whose post-detection SNR is denoted as γ_u, $P_{n,u}$ is the power of the nth transmitted symbol of the uth user, and $\hat{h}_{n,u}$ is the channel frequency response at the nth assigned subcarrier of the uth user. The geometrical interpretation of the achievable sum rate in the multiuser SC-FDMA system can be straightforward interpreted as performing multiuser EGP allocation in the system, where each user, subject to a given transmit power constraint, performs EGP allocation in the assigned set of subcarriers. It can be proven that $C_{\text{SC-FDMA,MU}}^{\text{EP, Independent}} \le C_{\text{OFDMA,MU}}^{\text{EP}} = \sum_{u=1}^{U}\sum_{n=0}^{N_u-1}\log_2(1+(|\hat{h}_{n,u}|\cdot P_{n,u})/N_0)$ by summing up the rate of all the users, each of which obeys (24), where the equality occurs when the channel frequency response at the assigned sub-carriers of each user is equal; that is, each user experiences flat fading among the assigned subcarriers for communication but the channel power gains can be different for different users. Note that the optimal multi-user waterfilling solution tends to exploit multi-user diversity and schedule at any time and any subcarrier of the user with the highest sub-carrier power gain-to-noise ratio to transmit to the BS. Consequently, from the system point of view, only the relatively strong sub-carriers, possibly from different users, are selected and the relative weak ones are avoided. In other words, each user is only assigned a set of relative strong sub-carriers. It will be a good choice if the above sub-carrier allocation scheme is applied for each user in SC-FDMA systems, because it is essentially equivalent to performing EGP among the relative strong sub-carriers for each user. As the number of users increases, the weak sub-carriers can be more effectively avoided due to the multi-user diversity. As a result, the effective channel for each user becomes less frequency selective, and the rate loss in SC-FDMA compared to OFDMA becomes smaller. The same effect happens if the BS is equipped with multiple antennas to exploit the spatial diversity to harden the channels. For SC-FDMA with the localized mapping constraint or the equidistantly distributed mapping constraint, multi-user diversity may help to reduce the rate loss with respect to an OFDMA system but with less degrees of freedom because multi-user diversity cannot guarantee that good sub-carriers assigned to each user are adjacent to each other or equidistantly distributed in the entire bandwidth. In this case, spatial diversity is much more important because it can always reduce frequency selectivity of each user's channel by using, for example, a maximum ratio combiner (MRC) at the receiver. As a result, the user specific resource allocation has less influence on the achievable rate no matter which sub-carriers are selected by the users but only the number of sub-carriers assigned to each user is needed to be considered. Consequently, not only is the rate loss mitigated but also the multi-user resource scheduler is greatly simplified. As an additional advantage, SC-FDMA can offer lower PAPR than OFDMA with negligible rate loss.

Table 1: Parameter assumptions for simulation

Parameters	Assumption
Carrier frequency	2.0 GHz
Transmission bandwidth	1.25 MHz, 2.5 MHz, 5 MHz, 10 MHz, 15 MHz and 20 MHz
Subcarrier spacing	15 KHz
Number of subcarriers in the system	75, 150, 300, 600, 900 and 1200
Number of subcarriers per RB	12
Channel model	3GPP SCME urban macro [14]
Number of UEs	up to 6
Number of BSs	1
Antennas per UE	1
Antennas per BS	1, 2, 3
BS antenna spacing	10 wavelengths
UE velocity	10 m/s

5. Simulation Results

In this section, we evaluate the performance of SC-FDMA in terms of the average achievable rate in LTE uplink scenario according to Table 1, along with specific comparison with OFDMA. In the simulation, time slots are generated using the SCME "urban macro" channel model [14]. The total numbers of the available sub-carriers in the system are assumed to be 75, 150, 300, 600, 900, and 1200 with the same sub-carrier spacing of 15 KHz, which correspond to the 1.25 MHz, 2.5 MHz, 5 MHz, 10 MHz, 15 MHz, and 20 MHz bandwidth system defined in LTE, respectively. These sub-carriers are grouped in blocks of 12 adjacent sub-carriers, which are the minimum addressable resource unit in the frequency domain, also termed a resource block (RB). For simplicity, we assume that each RB experiences the same channel condition, and for simulation its channel frequency response is represented by the 6th sub-carrier of that RB. We further assume that the transmit power is equally divided in all the transmitted components and decoding performs independently among the received block. In all the simulations, the resulting achievable system sum rate is normalized by the corresponding system bandwidth; that is, system spectral efficiency (bits/s/Hz) is used as a metric for performance evaluation.

First we evaluate the impact of the used bandwidth on system spectral efficiency. We consider a single user system where all the available subcarriers in the system are occupied by the single user. Figure 4 compares the

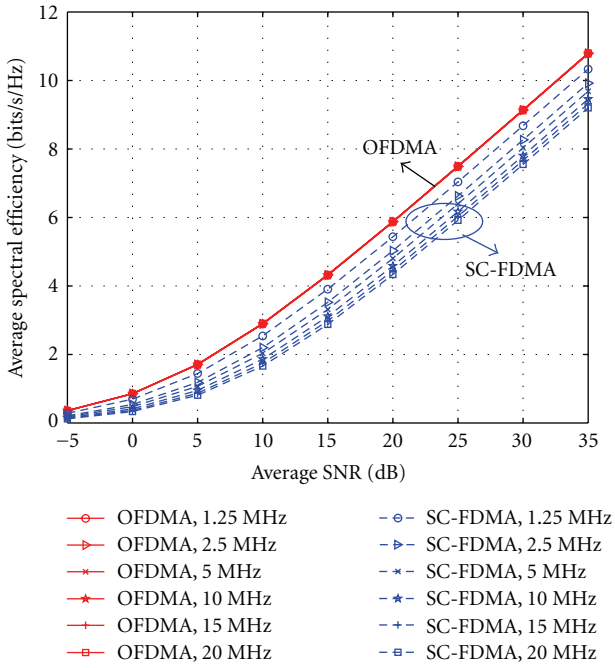

Figure 4: Comparison of the achievable information rate between OFDMA and SC-FDMA for different bandwidths under different average receive SNR conditions in the SCME "urban-macro" scenario with a single user in the system.

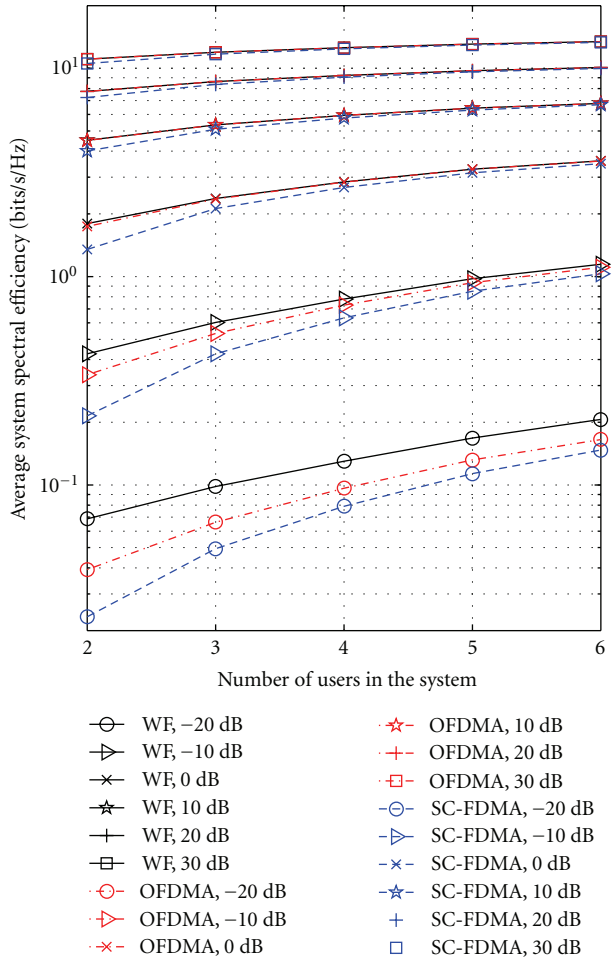

Figure 5: Comparison of the achievable system information rate between OFDMA and SC-FDMA for different numbers of users under different receive SNR conditions in SCME "urban-macro" scenario.

achievable average spectral efficiency between OFDMA and SC-FDMA for different transmission bandwidths under different average receive SNR conditions. It can be observed clearly that for the same average receive SNR, the average spectral efficiency for SC-FDMA is always smaller than that for OFDMA, which agrees very well with the analytical result presented in Section 3.1. Moreover, the achievable rate for OFDMA almost remains constant for different transmission bandwidths, while for SC-FDMA it decreases as the transmission bandwidth increases. This may due to the fact that as the transmission bandwidth increases and when it is much larger than the coherence bandwidth, each time slot consists of a similar number of weak subcarriers. Since the SC-FDMA rate is mainly constrained by channel deep fades (more power allocated for weak subcarriers and less power for good sub-carriers), having similar number of weak subcarriers for each time slot is less spectrally efficient than having more weak subcarriers for some time slots and less for the others, where the latter happens in the smaller bandwidth system with less frequency diversity. On the other hand, in the OFDMA system, transmit power is equally allocated in the used subcarriers; therefore, the achievable rate is insensitive to the distribution of the deep fades over different time slots.

Then we evaluate the impact of multi-user diversity on the system spectral efficiency. We assume that a number of users with the same transmit power constraints simultaneously communicate with the BS. Their path loss is compensated at the BS so that the average receive SNRs from all the users are the same, which varies from −20 dB to 30 dB in the 20 MHz bandwidth. First, the multi-user waterfilling (WF) algorithm [15] subject to the individual power constraint of the users is used to approximate the multi-user channel capacity, which gives a result close to the optimal power and subcarrier allocation solution for each user in the system. Then this subcarrier allocation solution which implicitly exploits multi-user diversity is adopted for simulations in both the OFDMA system and the SC-FDMA system but equal power allocation is used for the transmitted signal. Figure 5 plots the average system spectral efficiency over different numbers of users in both the SC-FDMA system and the OFDMA system under different receive SNR conditions. It can be seen that the average system spectral efficiency increases as the number of users in the system increases in both systems. Due to the multi-user diversity, the rate loss in SC-FDMA compared to OFDMA decreases as the number of users increases and it tends to disappear in high SNR conditions. It should be noted that the subcarrier allocation solution considered here is still suboptimal for both systems and a higher sum rate can be achieved in theory.

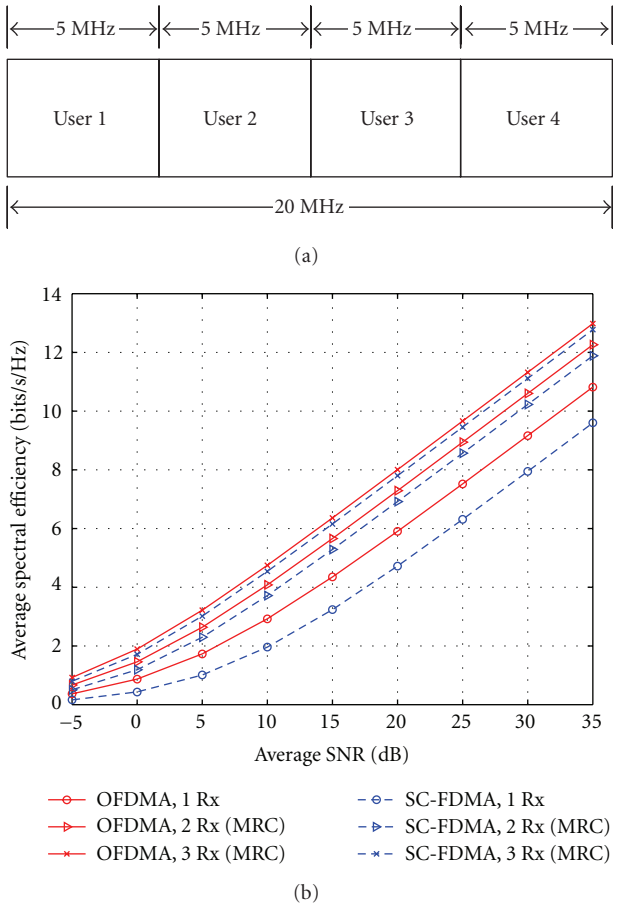

Figure 6: Comparison of the achievable information rate between OFDMA and SC-FDMA for different numbers of receive antennas in SCME "urban-macro" scenario. The system consists of 4 users with each occupying 5 MHz bandwidth.

Next, we evaluate the impact of spatial diversity on the system spectral efficiency. We consider that 4 users communicate simultaneously with the serving BS in the 20 MHz system, where each user occupies 5 MHz bandwidth as shown in the upper part of Figure 6. The number of receive antennas at the BS varies from 1 to 3. For multiple antennas, we assume that maximum ratio combining (MRC) is used in the frequency domain for both the SC-FDMA and OFDMA systems. It can be observed that as the number of receive antenna increases, the rate loss in SC-FDMA compared to OFDMA decreases significantly due to the channel hardening effect. Note that the simulation results have not taken into account the fact that SC-FDMA can further benefit from the lower PAPR property provided by the consecutive sub-carrier mapping for each user. Therefore, while being able to achieve a system sum rate very close to that in OFDMA, SC-FDMA has an additional lower PAPR advantage.

6. Conclusion

We have presented a framework for an analytical comparison between the achievable information rate in SC-FDMA and

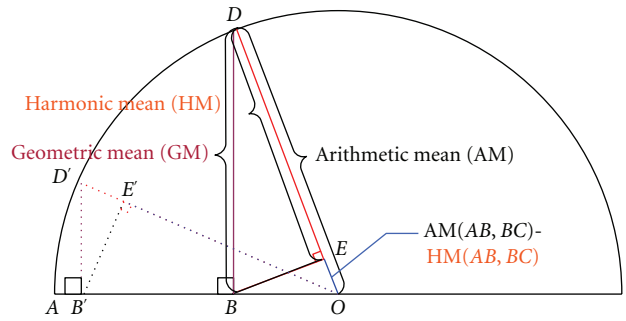

Figure 7: Geometrical interpretation of the harmonic mean, the arithmetic mean, and the geometric mean of $AB(AB')$ and $BC(B'C)$.

that in OFDMA. Ideally, SC-FDMA can achieve the same information rate as in OFDMA since DFT and IDFT are information lossless; however, proper coding across the transmitted signal components and decoding across the received signal components have to be used. We further investigated the achievable rate if independent capacity achieving AWGN codes is used and accordingly decoding is performed independently among the received components for SC-FDMA, assuming equal power allocation of the transmitted signal. A rate loss compared to OFDMA was analytically proven in the case of frequency selective channels, and the impact of the weak sub-carriers on the achievable rate was discussed. We also showed that the achievable rate in SC-FDMA can be interpreted as performing EGP allocation among the assigned sub-carriers in the nonprecoded OFDMA systems which has a similar geometrical interpretation with waterfilling. More importantly, it was pointed out and shown in 3GPP-LTE uplink scenario that the rate loss could be mitigated by exploiting multi-user diversity and spatial diversity. In particular, with spatial diversity we showed that while being able to achieve a system sum rate very close to that in OFDMA, SC-FDMA provides an additional lower PAPR advantage.

Appendices

A. Properties of the Circulant Matrix

Fact 1 ([16], Diagonalization of a circulant matrix). Denote $\mathbf{a}$ by the first column of a $Q \times Q$ circulant matrix $\mathbf{A}$ and $\mathrm{diag}\{\cdot\}$ by the diagonal matrix with the argument on the diagonal entries, then $\mathbf{A}$ can be diagonalized by pre- and postmultiplication with a Q-point FFT and IFFT matrices, that is, $\mathbf{F_Q A F_Q^H} = \mathbf{B} = \sqrt{Q}\,\mathrm{diag}\{\mathbf{F_Q a}\}$, where $\mathbf{B}$ is a $Q \times Q$ diagonal matrix with diagonal entries being a scale version of the Fourier transform of $\mathbf{a}$.

Fact 2. Because FFT and thus its matrix $\mathbf{F_Q}$ is invertible, it follows from Fact 1 that

$$\mathbf{A} = \underbrace{\mathbf{F_Q^H B F_Q}}_{\text{circulant }\{\mathbf{a}\}}, \tag{A.1}$$

where circulant $\{\mathbf{a}\}$ denotes a circulant matrix with the first column $\mathbf{a}$. Equation (A.1) means that a circulant matrix can be written as a multiplication of IFFT matrix, diagonal matrix, and FFT matrix. In particular, if and only if all entries of $\mathbf{B}$ are equal, then $\mathbf{A} = \mathbf{B}$ holds which is also a diagonal matrix with equal entries.

B. Geometrical Interpretation of the Harmonic Mean, the Arithmetic Mean, and the Geometric Mean

Suppose that we want to find out the harmonic mean of two values, represented by the length of AB and BC ($AB < BC$), respectively. By constructing a semicircle with radius $OC = (AB + BC)/2$ as depicted in Figure 7, the harmonic mean follows directly from the right-angled triangle DBO and DBE, where the length of DE equals the harmonic mean of AB and BC, denoted by $HM(AB,BC)$. It can be observed that $HM(AB,BC)$ is comparable to AB, the smaller value of the two. In order to show the sensitivity of harmonic mean to a small value, we can make AB much smaller than BC but keep $AB + BC$ fixed so that we can use the same semicircle to find their harmonic mean. Suppose that AB now becomes AB' and BC becomes $B'C$ as depicted in Figure 7, following the same way the harmonic mean of AB' and $B'C$, that is, $HM(AB',B'C)$ is given by $D'E'$. It can be seen that $D'E'$ is almost comparable to AB' which is the smaller value of the two. Therefore, the conclusion can be drawn that the harmonic mean is mainly constrained by the smaller value AB' although $B'C$ is much larger than AB'. For comparison purpose, the arithmetic mean and geometric mean of $AB(AB')$ and $BC(B'C)$, denoted by $DO(D'O)$ and $BD(B'D')$, respectively, are also drawn in Figure 7. It can easily be seen that if $AB = BC$, their harmonic mean is equal to their arithmetic mean and geometric mean.

References

[1] D. Falconer, S. L. Ariyavisitakul, A. Benyamin-Seeyar, and B. Eidson, "Frequency domain equalization for single-carrier broadband wireless systems," *IEEE Communications Magazine*, vol. 40, no. 4, pp. 58–66, 2002.

[2] N. Wang and S. Blostein, "Comparison of CP-based single carrier and OFDMA with power allocation," *IEEE Transactions on Communications*, vol. 53, no. 3, pp. 391–394, 2005.

[3] T. Shi, S. Zhou, and Y. Yao, "Capacity of single carrier systems with frequency-domain equalization," in *Proceedings of the 6th IEEE Circuits and Systems Symposium on Emerging Technologies: Frontiers of Mobile and Wireless Communication (CAS '04)*, vol. 2, pp. 429–432, Shanghai, China, May-June 2004.

[4] H. G. Myung, "Introduction to single carrier FDMA," in *Proceedings of the 15th European Signal Processing Conference (EUSIPCO '07)*, Poznan, Poland, September 2007.

[5] H. Ekström, A. Furuskär, J. Karlsson, et al., "Technical solutions for the 3G long-term evolution," *IEEE Communications Magazine*, vol. 44, no. 3, pp. 38–45, 2006.

[6] 3GPP TR 25.814, "3GPP TSG RAN physical layer aspect for UTRA," v7.1.0.

[7] V. Jungnickel, T. Hindelang, T. Haustein, and W. Zirwas, "SC-FDMA waveform design, performance, power dynamics and evolution to MIMO," in *Proceedings of the IEEE International Conference on Portable Information Devices (PIDs '07)*, Orlando, Fla, USA, March 2007.

[8] H. G. Myung, J. Lim, and D. J. Goodman, "Single carrier FDMA for uplink wireless transmission," *IEEE Vehicular Technology Magazine*, vol. 1, no. 3, pp. 30–38, 2006.

[9] W. Yu and J. M. Cioffi, "Constant-power waterfilling: performance bound and low-complexity implementation," *IEEE Transactions on Communications*, vol. 54, no. 1, pp. 23–28, 2006.

[10] L. Hoehn and I. Niven, "Averages on the move," *Mathematics Magazine*, vol. 58, no. 3, pp. 151–156, 1985.

[11] S. Cuomo, *Pappus of Alexandria and the Mathematics of Late Antiquity*, Cambridge University Press, Cambridge, UK, 2000.

[12] H. Wu and T. Haustein, "Radio resource management for the multi-user uplink using DFT-precoded OFDM," in *Proceedings of the IEEE International Conference on Communications (ICC '08)*, pp. 4724–4728, Beijing, China, May 2008.

[13] R. S. Cheng and S. Verdú, "Gaussian multiaccess channels with ISI: capacity region and multiuser water-filling," *IEEE Transactions on Information Theory*, vol. 39, no. 3, pp. 773–785, 1993.

[14] D. S. Baum, J. Hansen, G. Del Galdo, M. Milojevic, J. Salo, and P. Kyösti, "An interim channel model for beyond-3G systems: extending the 3GPP spatial channel model (SCM)," in *Proceedings of the 61st IEEE Vehicular Technology Conference (VTC '05)*, vol. 2, pp. 3132–3136, Stockholm, Sweden, May-June 2005.

[15] C. Zeng, L. M. C. Hoo, and J. M. Cioffi, "Efficient water-filling algorithms for a Gaussian mutliaccess channel with ISI," in *Proceedings of the IEEE Vehicular Technology Conference (VTC '00)*, Boston, Mass, USA, September 2000.

[16] G. H. Golub and C. F. van Loan, *Matrix Computations*, The Johns Hopkins University Press, Baltimore, Md, USA, 3rd edition, 1996.